Spectrotemporal dynamics of a picosecond OPO based on chirped quasi-phase-matching

D. Descloux, C. Laporte, J.B. Dherbecourt, J.M. Melkonian, M. Raybaut, C. Drag, A. Godard

Spectrotemporal dynamics of a picosecond OPO based on chirped quasi-phase-matching

D. Descloux,[1] C. Laporte,[1] J.-B. Dherbecourt,[1] J.-M. Melkonian,[1] M. Raybaut,[1] C. Drag,[2] and A. Godard[1,*]

[1]*ONERA–The French Aerospace Lab, F-91123 Palaiseau cedex, France*

[2]*Laboratoire Aimé–Cotton, Center national de la recherche scientifique, Université Paris-Sud, École normale supérieure de Cachan, F-91405 Orsay cedex, France*

**Corresponding author: antoine.godard@onera.fr*

We report on the first experimental investigation of the spectral dynamics of a synchronously pumped optical parametric oscillator (OPO) by use of dispersive Fourier transformation. For standard pumping rates, we observe a reproducible steady-state pulse-to-pulse spectrum. However, at high pumping levels, the OPO delivers pulse trains with nontrivial oscillatory spectral patterns. So as to benefit from a tailored broadband gain spectrum, the investigated OPO contains a chirped quasi-phase matching (QPM) nonlinear crystal. We explore the specific impacts of using such a remarkable parametric amplification medium where nonlinearly coupled frequencies vary with position. Depending on the QPM chirp rate sign, a red- or blue-shift of the emitted wavelength occurs when the OPO is switched on, leading to different spectral steady-states. These singular spectrotemporal dynamics are evidenced and explained for the first time.

Chirped quasi-phase-matching (QPM) nonlinear crystals offer unique features compared to conventional quadratic nonlinear materials. Indeed, one can engineer the phase-matched wavelengths as functions of the position z along the propagation axis in the material, the QPM grating period $\Lambda(z)$ being a function of z.

Owing to this versatile property, remarkable frequency conversion capabilities were demonstrated for optical parametric chirped pulse amplification [1], nonlinear pulse compression [2], or adiabatic frequency conversion [3,4]. Such materials can also be used as a broadband amplification medium in an oscillator. For a given nonlinear crystal length, the gain bandwidth can indeed be chosen with an appropriate QPM chirp rate $\kappa'(z)$, defined as the rate of change of the grating wavenumber, $K_g(z) = 2\pi/\Lambda(z)$, in the axial direction:

$$\kappa'(z) = -\frac{dK_g(z)}{dz}. \tag{1}$$

For instance, femtosecond optical parametric oscillators (OPO) were realized to benefit from the wide gain-bandwidth offered by chirped QPM [5,6]. However, due to the broadband spectrum of the femtosecond pump pulses, a simple physical picture is difficult to get since different frequencies of the pump spectrum can be involved at different positions in the crystal. A nanosecond OPO was also reported with remarkable spectral properties in transient and steady-state regime [7]. In particular, the authors observed a strong influence of the sign of the QPM chirp rate on the emitted spectrum that was not noticed with femtosecond OPOs. However, no clear explanation of this chirp rate sign dependence was provided so far.

In order to investigate these questions, we report here on the experimental and numerical investigations of the temporal characteristics of the spectrum emitted by a picosecond OPO based on a chirped QPM nonlinear material. For the first time, we investigate the pulse-to-pulse evolution of the spectrum emitted by a synchronously pumped OPO (SPOPO) during buildup of the oscillation, as well as in the steady-state regime. Depending on the sign of the QPM chirp rate, we observe red- or blue-shifts of the emitted wavelength, leading to different spectral steady-states. Owing to the narrow linewidth of the picosecond pump, each position in the crystal can now be linked to a single couple of signal-idler wavelengths. The observed effects are modeled and successfully interpreted in terms of position-dependent saturation effects, enabling to get a better understanding of the spectrotemporal dynamics of optical oscillators based on this unique class of nonlinear materials.

We also evidence nontrivial oscillatory spectral patterns for high pumping rates, instead of a stable steady-state spectrum. These latter spectral behaviors are also expected to occur in SPOPOs based on conventional nonlinear crystals and should be taken into consideration for the design of efficient optical oscillators with proper spectral properties.

To carry out such an experimental study, which is made challenging due to the high pulse repetition rate of SPOPOs (usually several tens of MHz), we implement dispersive Fourier transformation by use of a comparable approach as the one reported in [8] to measure the pulse-to-pulse spectrum emitted by supercontinuum sources. The output signal beam is coupled to a highly dispersive optical fiber, and the spectrum is thus temporally dispersed and can be recorded by use of a high-speed photodetector at the output end of the fiber.

The experimental setup is shown in Fig. 1. A singly resonant SPOPO is pumped by a picosecond Nd:YVO_4 mode-locked laser with a 76-MHz repetition rate (High-Q), delivering pulses of 8 ps at 1.064 μm. The SPOPO is based on an AR-coated, 60-mm-long, MgO-doped aperiodically poled lithium niobate (APPLN) crystal (HC Photonics). Experiments are carried out with a

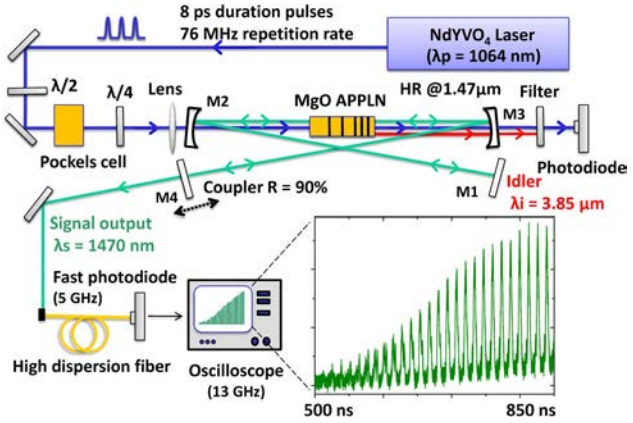

Fig. 1. Schematic diagram of the experimental setup; inset: example of recorded oscilloscope trace of OPO signal during buildup of the oscillation.

QPM grating with a linear component of the chirp rate of $\kappa' = 3.9 \times 10^4$ m^{-2} (single pass parametric gain bandwidth of 15 nm) and a central signal wavelength of 1.47 µm, operating at 80°C. To reduce amplitude ripples in the parametric gain spectrum, the chirped QPM pattern is apodized following a similar approach as the one described in [9,10]. The SPOPO resonator has a standing-wave configuration with a central focused arm between two collimated arms. The radius of curvature of both spherical mirrors, M2 and M3, is 500 mm, resulting in an estimated signal waist radius at $1/e^2$ of 150 µm. Mirrors M1, M2, and M3 are highly reflective at the signal wavelength; the plane output coupler M4 has a reflectivity of 90% at the signal. The pump beam is focused in the middle of the crystal with a waist radius of 110 µm. To change the sign, positive or negative, of the QPM chirp rate, we flip the orientation of the APPLN crystal in the cavity.

For both orientations, the cavity length is set to minimize the oscillation threshold and kept the same for the experiments presented in the following. The corresponding threshold power is 1 W. The quantum conversion efficiency increases from threshold up to a constant value of 27%, reached for a pumping rate of five.

To carry out the spectral characterization, we use two highly dispersive fibers (SMF-DK, OFS): fiber A inducing a group delay dispersion (GDD) of −2000 ps/nm and fiber B introducing a GDD of −500 ps/nm at the central signal wavelength around 1.47 µm. Since the oscilloscope (LeCroy) bandwidth is 13 GHz, the detection bandwidth of the system is limited by the 5-GHz bandwidth of the fast photodiode (SIR5, Thorlabs) and the GDD of the fiber, leading to a spectral resolution of about 0.1 nm for fiber A and of about 0.4 nm for fiber B. The spectrum acquisition window is imposed by the GDD of the fiber and the pulse repetition rate of 76 MHz to a 6.5 nm span with fiber A and to a 26 nm span with fiber B. Hence, fiber B is useful when aliasing occurs with fiber A, enabling to analyze broader spectra at the price of a lower resolution.

The investigation of the spectrotemporal dynamics upon buildup of the SPOPO oscillation is made possible by use of a Pockels cell that enables to rapidly switch-on the pump, by changing its polarization at the OPO input. The switching time is less than twice the repetition period, i.e., 26 ns. The inset in Fig. 1 shows a typical pulse train recorded at the output of the dispersive fiber when the OPO is pumped three times above threshold. One can clearly see the dynamics of the oscillation buildup just before the OPO reaches its steady-state.

Figure 2 shows a sequence of pulse-to-pulse spectra, recorded with fiber A, for successive cavity round-trips in the steady-state regime when the APPLN crystal orientation is set to have a negative chirp rate. The emitted spectrum is almost identical from one pulse to another and is consistent with the average spectrum recorded with an optical spectrum analyzer (OSA) (Ando, resolution 15 pm). In both cases, the spectra have an asymmetric shape with a main peak and side lobes on one side. We can nevertheless notice, comparing the traces, a difference concerning the dynamic range whose possible origin could be nonlinearity of the fast detector or nonlinear phenomena in the dispersive fiber. Indeed, the response of the detector is not specified to be linear over its full dynamic range. Regarding nonlinear effects in the fiber, we typically inject a peak power lower than 90 mW to have a good signal-to-noise ratio at low powers. This actually corresponds to a ratio of the dispersion length to the nonlinear length of 0.1 at the input of the fiber. This value is small but not negligible, meaning that some nonlinear effects could occur and enlarge the spectra [11]. Nevertheless, the initial pulse duration of 5 ps is rapidly enlarged due to dispersion (the duration is doubled within 230 m, while the typical fiber length is of several kilometers). The nonlinear effects are thus expected to rapidly decrease during propagation. Despite this residual distortion that could be removed with an improved setup, the measurement technique provides information on the pulse-to-pulse evolution of the spectrum which is not accessible with an OSA.

Figure 3(a) shows an example of the experimental pulse-to-pulse spectrum recorded during oscillation buildup up to steady-state for a negative chirp rate. From one recording to the other (not shown here), the first detectable spectra can display different features reminiscent of the initial parametric fluorescence spectra.

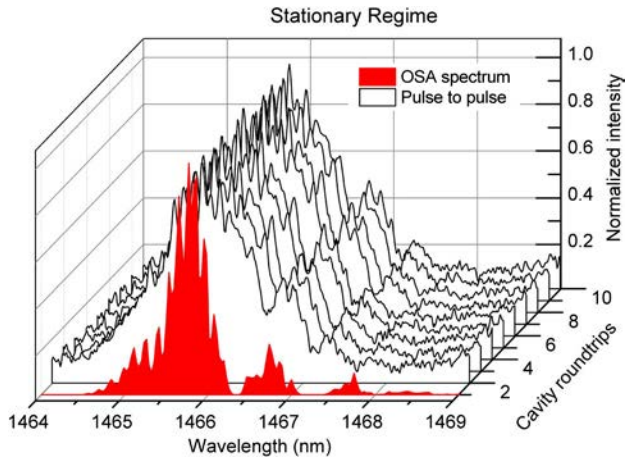

Fig. 2. Steady-state pulse-to-pulse spectrum, for a negative chirp rate, emitted when the OPO is pumped three times above threshold (black lines) and average spectrum recorded with an optical spectrum analyzer (red filled area).

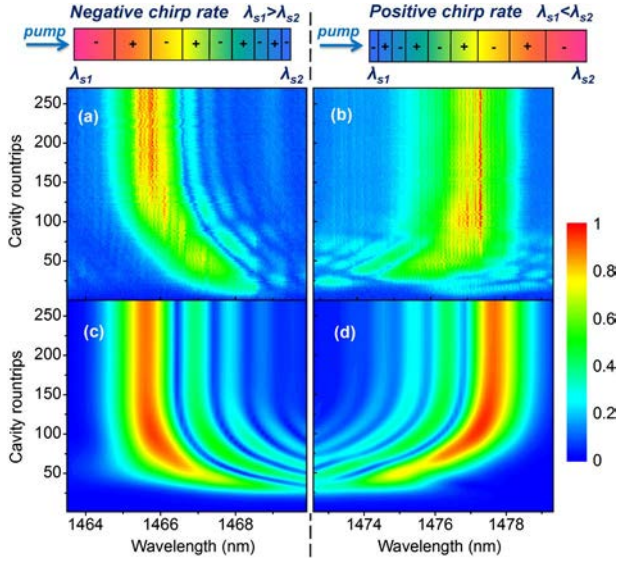

Fig. 3. Spectrograms of the signal spectrum as a function of the cavity round trips upon buildup of the oscillation when the OPO is pumped three times above threshold: (a) and (c) are, respectively, experiment and modeling for a negative QPM chirp rate; (b) and (d) are, respectively, experiment and modeling for a positive QPM chirp rate. Schematic diagrams of chirped QPM crystal with different chirp rate sign are shown on the top: the evolution of signal wavelengths phase-matched at the input end λ_{s1} and output end λ_{s2} of the crystal are represented with color, the plus and minus signs represent the nonlinear susceptibility inversion, and the arrows indicate the pump beam propagation direction.

However, they always evolve toward a steady-state spectrum very similar to the one shown in Fig. 2. One should also notice that, in contrast to what is expected for uniform QPM [12], a spectral shift occurs during buildup of the oscillation. Moreover, as shown in Fig. 3(b), one observes a red shift for a positive QPM chirp rate instead of the blue shift in Fig. 3(a) for a negative QPM chirp rate, leading to a steady-state spectrum that also depends on the chirp rate sign. We measure the pulse-autocorrelation traces for both chirp signs (not shown here). They both show a regular single-peak profile with a FWHM of 7.5 ps.

To have a better understanding of these spectral behaviors, specific to chirped QPM, we also perform numerical modeling of the SPOPO pulse-to-pulse spectra. For that purpose, we use a homemade plane-wave simulation code based on a finite difference method in temporal domain to solve the coupled nonlinear equations, taking into account group velocity mismatch and dispersion [13]. To initiate parametric generation, we consider initial idler and signal pulses of weak intensity, equal to half a photon in each longitudinal mode contained in a schematic cylindrical mode, and with a spectrum broader than the parametric gain bandwidth.

As shown in Figs. 3(c) and 3(d), the simulations are consistent with experiments and predict a shift of the OPO spectrum while reaching the steady-state regime. In modeling, the initial spectrum is very large: its width corresponds to the crystal gain bandwidth. Experimentally, we are not able to observe such a broad initial spectrum because of the very low corresponding peak power. The differences between measurements for positive and negative chirps, not recovered by modeling, may be due to phenomena that are not considered in our model, e.g., higher order nonlinear processes or non-collinear effects [14]. However, these effects are not expected to be dominant regarding the moderate peak intensity and the stable Gaussian beam profile for both chirp signs (not shown here). A good qualitative agreement is indeed obtained between experiment and modeling: we observe the same effect of the QPM chirp rate sign on the shift direction. We can also notice that the measured and calculated buildup times are comparable.

To understand the influence of the QPM chirp on the SPOPO spectral features, we analyze the simulated peak parametric gain spectra for small and strong incident signal, corresponding, respectively, to the early phase of the oscillation buildup and to the steady-state regime. To obtain such gain spectra, we calculate the single-pass gain of signal pulses (5 ps duration with a Fourier transform limited linewidth of 0.64 nm) varying the pulse central wavelength across the full gain bandwidth. On the one hand, for small signal regime [see Fig. 4(a)], the wavelengths amplified in the crystal input end are favored owing to a longer interaction length. But, on the other hand, for a strong signal [see Fig. 4(b)], saturation of the peak parametric gain–that leads to pump reconversion–occurs for the wavelengths initially favored, while the wavelengths amplified in the output end of the crystal now experience less saturation. Comparable effects are obtained for both chirp rate signs, which is consistent with the shift toward the wavelength amplified at the output end of the crystal while reaching stationary regime in Fig. 3.

The calculated gain spectra are also qualitatively consistent with the main feature of the OPO spectrum with side lobes of smaller intensity. However, the peaks do not necessarily superimpose to the local maxima of the gain spectrum. Those features might be linked with the subtle evolution of the nonlinear phase into the crystal and cannot be understood if one considers only the single-pass parametric gain spectrum for incident signal pulses with narrow linewidth. Indeed, for broadband conversions, the nonlinear phase shows fast and complex evolution inside the crystal and for each part of the pulse in the time domain. This evolution leads to cycle of conversion and reconversion of energy from pump to signal and idler

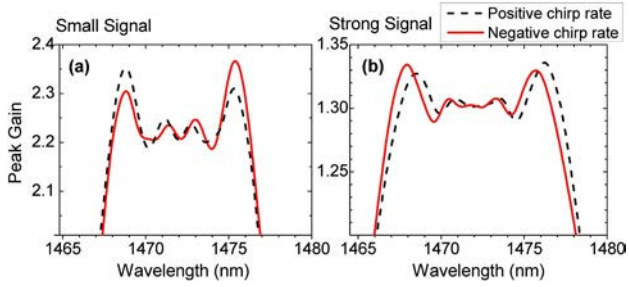

Fig. 4. Simulated peak-intensity parametric gain spectra for: (a) small signal (signal power × 1000 = pump power) and (b) strong signal (intracavity signal power = 1.7× pump power). Incident pump power is 1.5, the one considered in Fig. 3, i.e., equivalent to 4.5× threshold, to enhance the effects for more visual clarity.

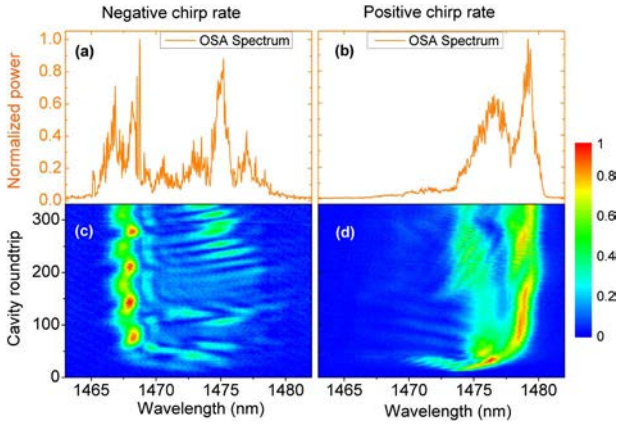

Fig. 5. Spectrograms of the signal spectrum as a function of the cavity round trips upon buildup of the oscillation for negative (c) and positive (d) chirp rate and the OSA spectrum corresponding for negative (a) and positive (b) chirp rate. The OPO is pumped seven times above threshold.

during the propagation along the crystal length, which is not the same for each spectral component of the pulse.

We also carry out experiments at higher pumping levels. We first observe a broadening of the emitted spectrum that is consistent with modeling. Figs. 5(a) and 5(b) show the corresponding average spectra of the signal emission for both chirp rates sign, for a pumping rate of seven times above threshold, recorded by use of the OSA. Then, we use fiber B to observe the real-time evolution of those broadband spectra with a sufficient span. As shown in Figs. 5(c) and 5(d), owing to our pulse-to-pulse acquisition setup, we observe fast modulations of the spectra that occur for this high pumping rate. Those variations of the energy repartition between the spectral components of each pulse cannot be perceived with OSA measurements. The QPM chirp sign dependence of the spectra shown in Fig. 5 is analogous to what is observed at lower pump powers. However, the oscillatory spectral patterns, without a constant steady state, are consistent with spectral evolution previously predicted by extensive modeling of SPOPOs based on uniform QPM [12]. These dynamical spectral behaviors are thus expected to occur as well with other SPOPO devices based on conventional nonlinear crystals. Soliton formation can also lead to oscillatory regime in SPOPOs [15] and could be valuably investigated by use of a similar measurement technique.

In conclusion, we have investigated for the first time the spectrotemporal properties of a SPOPO. These measurements have been carried out owing to a dispersive-Fourier-transformation device based on a highly dispersive fiber and a fast detector that enable to observe SPOPO pulse-to-pulse spectra. This setup has then been associated to a Pockels cell enabling the investigation of the buildup regime of our SPOPO based on chirped QPM. Depending on the sign of the QPM chirp rate, we evidence red- or blue-shifts of the emitted wavelength, leading to different spectral steady-states. These previously unknown spectrotemporal effects are modeled and successfully interpreted in terms of parametric gain saturation effects, particular to chirped QPM, providing a better understanding of OPOs based on this unique class of nonlinear materials. Further investigations on the influence of specific parameters such as high pumping rates or cavity length detuning could be of great interest, just as the study of other temporal regimes or QPM profiles. We also evidence that nontrivial oscillatory spectral patterns occur for high pumping rates, instead of a stable steady-state spectrum. These spectral features are expected to occur for SPOPO based on conventional quadratic nonlinear materials as well. The pulse-to-pulse spectrum measurement technique implemented here might thus become a useful tool for SPOPO developers and users to characterize extensively the output spectral properties.

We are grateful to Michel Lefebvre for critical reading of the manuscript and valuable suggestions. This work has been supported by Triangle de la physique (2011-028T-SAFIR) and "Laboratoire d'Excellence Physics Atom Light Mater"—LabEx PALM (SYCLOP) part of ANR Investissements d'Avenir (ANR-10-LABX-0039).

References

1. B. W. Mayer, C. R. Phillips, L. Gallmann, M. M. Fejer, and U. Keller, Opt. Lett. **38**, 4265 (2013).
2. M. A. Arbore, O. Marco, and M. M. Fejer, Opt. Lett. **22**, 865 (1997).
3. H. Suchowski, V. Prabhudesai, D. Oron, A. Arie, and Y. Silberberg, Opt. Express **17**, 12731 (2009).
4. C. R. Phillips and M. M. Fejer, Opt. Lett. **35**, 3093 (2010).
5. T. Beddard, M. Ebrahimzadeh, D. T. Reid, and W. Sibbett, Opt. Lett. **25**, 1052 (2000).
6. K. A. Tillman, D. T. Reid, D. Artigas, J. Hellström, V. Pasiskevicius, and F. Laurell, Opt. Lett. **28**, 543 (2003).
7. K. A. Tillman and D. T. Reid, Opt. Lett. **32**, 1548 (2007).
8. P. Kelkar, F. Coppinger, A. Bhushan, and B. Jalali, Electron. Lett. **35**, 1661 (1999).
9. M. Charbonneau-Lefort, B. Afeyan, and M. M. Fejer, J. Opt. Soc. Am. B **25**, 463 (2008).
10. C. R. Phillips, C. Langrock, D. Chang, Y. W. Lin, L. Gallmann, and M. M. Fejer, J. Opt. Soc. Am. B **30**, 1551 (2013).
11. G. P. Agrawal, *Nonlinear Fiber Optics (Optics and Photonics)*, 5th ed. (Academic, 2013).
12. D. T. Reid, Opt. Express **19**, 17979 (2011).
13. G. Arisholm, Opt. Express **15**, 6513 (2007).
14. M. Charbonneau-Lefort, B. Afeyan, and M. M. Fejer, J. Opt. Soc. Am. B **25**, 1402 (2008).
15. D. T. Reid, J. M. Dudley, M. Ebrahimzadeh, and W. Sibbett, Opt. Lett. **19**, 825 (1994).